



## Research paper

# Offshore wind support structures – Evaluation of size effects and influencing factors on the fatigue performance of butt-welded joints using an updated database

H. Bartsch<sup>a</sup>, S. Röscher<sup>b</sup>, M. Braun<sup>c</sup>, J. Maljaars<sup>d</sup>, J. Schubnell<sup>e</sup>, M. Rauch<sup>f</sup>,  
A. Chahardehi<sup>g</sup>, A. Mehmanparast<sup>h,\*</sup>

<sup>a</sup> Institute of Steel Construction, RWTH Aachen University, Aachen, Germany

<sup>b</sup> Institute of Structural Design, University of Stuttgart, Germany

<sup>c</sup> DLR Institute of Maritime Technologies and Propulsion Systems, Geesthacht, Germany

<sup>d</sup> Eindhoven University of Technology, Eindhoven, Netherlands

<sup>e</sup> Fraunhofer Institute for Mechanics of Materials IWM, Freiburg, Germany

<sup>f</sup> Hochschule Kaiserslautern, Kaiserslautern, Germany

<sup>g</sup> Kent Energies, London, United Kingdom

<sup>h</sup> University of Strathclyde, Glasgow, United Kingdom

## A B S T R A C T

Offshore wind turbine support structures, such as monopiles, require high fatigue resistance at welded connections, particularly around the circumferential welds. This paper reviews the influence of plate thickness on the fatigue performance of welded butt joints and presents a statistical evaluation of relevant fatigue test data. The analysis combines the European fatigue database (DAST Database) with newly available data related to welded offshore wind structures to ensure representativeness for modern monopile structures. The unfiltered European fatigue database contains more than 4700 data points for butt welds, but its heterogeneity in materials, welding processes, and specimen geometries produces a large scatter. After filtering for offshore wind-relevant conditions, by including thick plates ( $t \geq 25$  mm), various sub-grades of S355 structural steel, double-sided butt welds, submerged arc welding, axial loading condition, and load ratios of  $R \geq 0$  the dataset reduces drastically but yields consistent results based on relevant test data. In this subset, the characteristic fatigue resistance corresponds to FAT 90, while the inverse slope of the S–N curve increased to  $m \approx 3.45$ , which is higher than the EN 1993-1-9 standard assumption of  $m = 3$  but in excellent agreement with the monopile-specific D curve in DNV-RP-C203 standard. The newly added offshore wind related datasets, particularly for plate thicknesses of 40 mm and 50 mm, confirm these findings. They demonstrate a fatigue life reduction trend with increasing the plate thickness for  $t \geq 25$  mm, while the thickness correction formulation in EN 1993-1-9 standard has been found to produce a trend that falls at the lower bound of the scatter. Moreover, the variations in the load ratios of  $R \geq 0$  and the yield strength in various sub-grades of S355 steel were found to have no significant influence on fatigue resistance. Overall, the results demonstrate that targeted filtering and integration of offshore wind-specific data provide a more realistic basis for fatigue design and life assessment of monopile support structures.

## 1. Introduction

### 1.1. Offshore wind structures and fatigue relevance

Climate change and raw material shortage are two of the global challenges that have a major impact on our built environment. The consequences, for example, concerning global warming can already be seen by intensified extreme weather events such as heavy rainfall and floods, intense heatwaves and droughts, or severe storms. To overcome the global challenges, the United Nations have set up 17 Sustainable Development Goals (United Nations). The construction industry can contribute to accomplish the Sustainable Development Goals, amongst

others, to ensure a safe, resilient and sustainable development of cities and communities, to build resilient infrastructure, as well as to assure affordable and green energy (United Nations). Wind energy and the circular economy are already of considerable significance and are expected to play an even more prominent role in meeting the growing global energy demand in conjunction with the sustainable utilisation of materials in the future. Ensuring the functionality of wind turbines across their entire life cycle is critical, with fatigue behaviour representing a particularly decisive factor. In Europe, for instance, wind energy is a key component of the European Green Deal to reduce at least 55% of the net greenhouse gas emissions by 2030 in comparison to 1990 and to reach climate-neutrality by 2050 (European Commission, 2019).

\* Corresponding author.

E-mail address: [ali.mehmanparast@strath.ac.uk](mailto:ali.mehmanparast@strath.ac.uk) (A. Mehmanparast).

<https://doi.org/10.1016/j.oceaneng.2026.124370>

Received 5 November 2025; Received in revised form 8 January 2026; Accepted 18 January 2026

Available online 28 January 2026

0029-8018/© 2026 The Authors. Published by Elsevier Ltd. This is an open access article under the CC BY license (<http://creativecommons.org/licenses/by/4.0/>).

The installed wind power capacity amounts to 285 GW at the end of 2024 in Europe, consisting of 248 GW by onshore (a share of 87%) and 37 GW by offshore wind turbines (a share of 13%) (Wind Europe, 2025). The outlook until 2030 expects an increase of the installed wind power capacity by 48 GW concerning offshore wind (a share of 25%) and by 187 GW in total (Wind Europe, 2025).

UK and Germany are the key players in Europe concerning offshore wind with a share of 44% and 25% of the installed offshore wind turbines, respectively. Offshore wind turbines (OWTs) are following a trend of increasing capacity, highlighting the industry's continued drive for greater efficiency and economies of scale, which is accompanied by a continuous growth in size of the turbines and subsequently the support structures. With the increase in turbine size and capacity, fatigue has become an increasingly governing factor in the design of the supporting structures. Optimized design concepts, especially regarding fatigue damage, are of particular interest with regard to an efficient and intelligent use of materials throughout the whole life cycle of offshore wind turbine structures (Wind Europe, 2025). The first generation of large-scale offshore wind farms, developed in the early 2000s, were typically designed for an operational life of 20–25 years. Based on this design horizon, several offshore wind farms in the UK and Denmark have now reached the end of their initially design life and have subsequently been decommissioned (Wind Europe, 2025). With more than 1000 offshore wind turbines across Europe expected to reach the end of their design life within the next decade, novel strategies for life extension, repowering, and decommissioning must be systematically evaluated in the coming years.

Offshore wind turbines exhibit an enormous potential compared to onshore despite the small share of total installations. Offshore wind farms are usually characterised by 60% full load hours, a high availability of large turbines, hardly any restrictions regarding turbine, and blade sizes which can help reduce the production costs and to lower energy costs (Fraunhofer, 2021). In future, a reliable grid integration, economic aspects, and technological development, such as turbine size as well as lifetime extension, play a crucial role taking advantage of the full potential of offshore wind (Fraunhofer, 2021).

### 1.2. Role of plate thickness with regards to fatigue life of offshore structures

To fulfil the growth target of the offshore wind energy market, economic and technological aspects are mainly affecting the decision making concerning future wind projects with the expectation that larger and thicker support structures will be used. Due to the high cyclic loading condition in the offshore environment, the service life of offshore wind turbine structures is strongly governed by their fatigue behaviour. Current investigations demonstrate that the geometry of butt welds has a significant influence on the fatigue performance and consequently on the service life of welded joints in offshore wind turbine support structures (Mehmanparast and Lotsberg, 2025). It is historically known that the thickness of a welded structure can influence its fatigue resistance (Pedersen, 2019). In thicker welded plates, the stress gradient at the weld toe is lower, but the relative sharpness of the weld toe angle may increase, potentially facilitating crack initiation (geometrical size effect) (Lotsberg, 2014). Larger welded structures can also experience higher residual stresses due to greater welding constraints which might not completely relax during loading and consequently might influence the fatigue life (technological size effect) (Farajian and Nitschke-Pagel, 2015). Furthermore, the likelihood of unfavourable weld bead geometries and inner imperfections can increase with weld length, while the probability of inner imperfections may increase with the numbers of welded layers, so the thickness and weld size may contribute to a higher risk of flaws and of fatigue failure (statistical size effect) (Pedersen, 2019; Lotsberg, 2014). On the other hand, misalignment induced secondary bending stresses are typically higher for thinner plated structures due to larger welding induced distortions in such structures (Mancini

et al., 2020). These aspects highlight the necessity of investigation regarding thickness effect to fulfil the growth target of the wind energy market in an economic, technologically advanced and sustainable way.

### 1.3. Scope and objective of the present study

Among the various welded details in offshore wind turbine structures, double-sided butt welds constitute one of the most fundamental structural connection types, currently and for the foreseeable future. These welds are widely employed in support structures, where they play a critical role in ensuring structural continuity and integrity under complex loading conditions. Among the various types of support structures, monopiles, which support the majority of existing offshore wind turbines worldwide, are fabricated using double-sided butt-welds for joining structural steel plates and require a comprehensive study regarding the continuously increasing turbine sizes. Given their exposure to dynamic environmental forces and cyclic loading, the performance of double-sided butt welds is particularly significant in governing the overall fatigue resistance, service life, and safety of offshore wind turbine support structures. The fatigue behaviour of various types of welds, including double-sided butt welds, has been extensively studied in the past; however, the existing databases lack systematic information on thickness effect, weld length effect, yield strength influence, mean stress influence, and welding process parameters for relevant steels employed in OWTs. In addition, understanding the statistical variability and the temporal trends in the historical fatigue data, spanning from early studies in the 1960s to more recent results, may obscure the potential improvements achievable with modern fabrication methods such as submerged arc welding (SAW), multilayer welds, and advanced quality control techniques. Consequently, the applicability of standard fatigue classes to large-scale offshore structures made from thick plates ( $\geq 50$  mm) requires a critical reassessment.

In order to address the current knowledge gaps, the aim of the present study is therefore to:

1. Review the current understanding of fatigue performance of welds in offshore welded structures using in-air data as the baseline, with a particular focus on the weld geometry and material data, as derived from the literature.
2. Analyse and refine existing fatigue test data from the European database (Feldmann et al., 2024) in order to identify how filtering for relevant parameters of weld geometry and fabrication (e.g. plate thickness, welding process) affects the statistical evaluation of fatigue resistance.

## 2. Weld geometry and its influence on fatigue resistance

### 2.1. General

The geometry of a weld has a profound influence on its fatigue performance. At the global level, the weld geometry is characterised by parameters such as weld width and height, throat thickness, penetration depth, and overall alignment, which show no large variation in automatic welding processes along the weld length and govern the distribution of stresses under cyclic loading. In contrast, the local geometry refers to small-scale features, such as the weld toe or local surface imperfections, including the weld toe radius, weld toe angle, depth of undercuts, imperfections, all of which may vary along the weld length. These local surface imperfections are particularly significant as they frequently act as preferential positions for fatigue crack initiation, thereby reducing the structural integrity and service life of the welded component. In the present study, attention is directed primarily towards the global aspects of weld geometry, as they provide a fundamental understanding of the macroscopic fatigue behaviour and are crucial for establishing reliable fatigue design guidelines; nevertheless, it is recognised that the influence of local geometry is equally significant.

Consequently, future studies are aimed to extend the current work by systematically addressing the effects of local weld geometry and surface imperfections, thereby offering a more comprehensive assessment of fatigue performance in offshore wind turbine structures.

### 2.2. Causes of size effects

Since it is practically impossible to conduct fatigue tests on full-scale monopiles, one has to rely on mechanical principles and extrapolation of smaller scale test data to evaluate the global aspects on the fatigue resistance. Monopile structures are manufactured by cold rolling and bending thick structural steel plates, which are welded longitudinally to form cans and subsequently welded circumferentially to achieve the required monopile length. Due to the large wall thickness, double-sided butt welds are used in automated fabrication. Under global loading of large-diameter monopiles, circumferential welds are prone to fatigue cracks perpendicular to the axial loading direction. Therefore, to understand fatigue crack initiation behaviour in monopiles with large diameters and thicknesses, fatigue test data from double-sided butt-welded plates subjected to axial loading are considered in representative laboratory-scale tests to replicate the cracking behaviour observed in full-scale monopile structures.

In evaluation of fatigue life of double-sided butt welded plates, the size effect refers to the combined effects of plate thickness  $t$ , distance between weld toes  $L$  (which is often referred to as weld width), and the weld length  $W$ , as schematically shown in Fig. 1.

Because the weld bead width  $L$  is approximately linearly related to the plate thickness  $t$  in butt welds, and the weld length  $W$  is linearly dependent on the diameter  $D$  of the monopile, the size effect parameters can be reduced to  $t$  and  $D$ . Based on the historic investigations such as (Gurney, 1979) and (Berge, 1984), it is well known that the fatigue resistance of a thick welded geometry can be lower than that of a thin welded geometry. Some explanations of the causes of thickness effects can be found e.g. in (Shams-Hakimi et al., 2017) and (Pedersen, 2019), which are summarised below:

- There are two geometrical factors related to  $t$  which can be considered as geometrical size effect: First, the stress gradient at the notch is larger for smaller values compared to larger values of  $t$ , as schematically shown in Fig. 2. Hence, in the stage of a physically long crack but still small in size, which dominates the fatigue life of a welded joint, a larger stress intensity factor is observed for a larger  $t$ . Second, the local geometry at the weld toe results from the weld bead at that location and it does not scale with  $t$ . For example, if the weld toe radius from weld to base material surface is 0.2 mm in two plates with thickness 10 mm and 100 mm, the ratio between weld toe radius and thickness is 0.02 and 0.002, respectively. Hence, from a relative point of view, the transition geometry would be different from the thinner to the thicker plate.
- There is a technological size effect, where the weld process and the residual stress might be different for small, compared to large, welded geometries. For complex welded structures, larger constraints to deformation during welding apply in larger welded geometries,

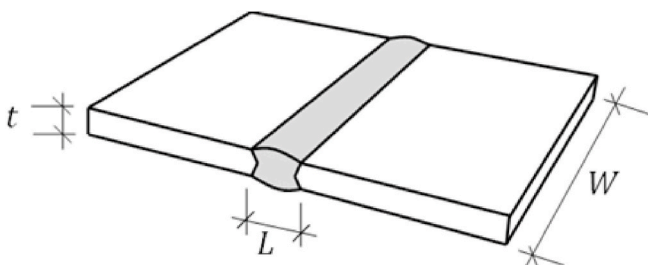


Fig. 1. Global weld geometry of the double-sided butt welds between plates.

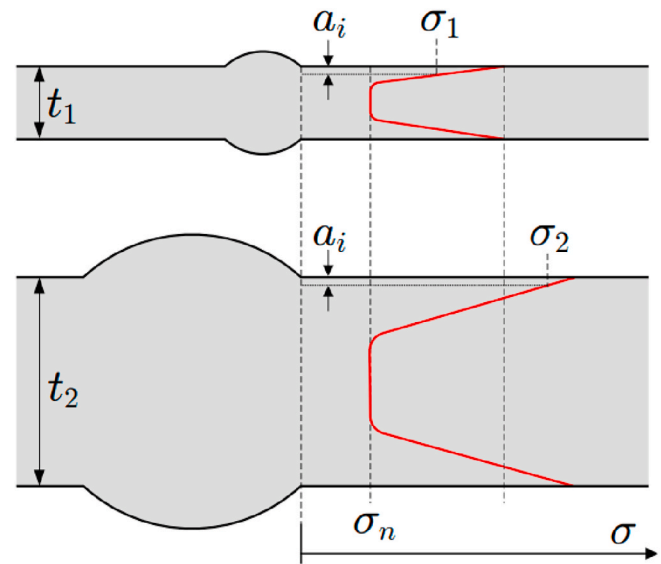


Fig. 2. Effect of plate thickness on stress gradient and fatigue behaviour (Berge, 1985).

resulting in higher absolute residual stresses. Subsequently, because of mean stress dependence, a higher extent of tensile residual stress reduces the fatigue life, hence this might have significant detrimental effects on fatigue life.

- There is a statistical size effect for weakest link failure modes such as fatigue. The probability of an unfavourable local geometry, such as a local undercut at a location with a local large weld toe angle, increases with the length of the weld. Considering the weld toe is the main location of crack initiation in a monopile butt weld, the statistical effect mainly depends on the diameter  $D$ .

In standards, the size effect is usually related to  $t$  (and  $L$ ), and not on  $W$  (or  $D$ ). Following a proposal by Gurney (1979) the effect of  $t$  on the fatigue resistance of butt-welded joints in standards is usually expressed as:

$$\Delta\sigma_C = \Delta\sigma_{C,ref} \cdot \left(\frac{t_{ref}}{t}\right)^k \tag{1}$$

where  $\Delta\sigma_C$  is the fatigue resistance of a welded structure with  $t > t_{ref}$ ,  $\Delta\sigma_{C,ref}$  is the fatigue resistance of a welded structure with a reference thickness  $t_{ref}$ , and  $k$  is the thickness exponent, equal to 0.2 in IIW-Recommendations (Hobbacher and Baumgartner, 2024) in as-welded state and in prEN 1993-1-9:2025 (2025) for butt welds. A similar equation, but by including the weld width as an additional parameter in calculation of the effective thickness, is recommended in DNV-RP-C203 (2025), which is most relevant for monopiles and therefore presented and discussed in Section 3.3 in detail.

### 2.3. Geometrical and technological size effects

Most studies on the geometrical size effect were conducted on cruciform joints or welded attachments, where a clear size effect is demonstrated. Regarding the geometrical size effect, however, a mild notch such as the one induced by a butt weld should have a smaller geometrical size effect, because the stress gradient is small and the notch effect caused by the weld toe geometry is limited. Indeed, a simulation using fracture mechanics of a ground flush joint confirms that  $t$  has very small or even no influence. Consequently, the recent update of the IIW recommendation for fatigue design of welded joints and components removes the thickness correction for flush ground joints (i.e.  $k = 0$ ) (Hobbacher and Baumgartner, 2024).

Three approaches are generally conducted to evaluate the size effect of butt-welded joints, namely, through testing, through fracture mechanics simulation and through evaluation of local stresses. Examples of evaluation of the thickness effect by local stresses (Livieri and Tovo, 2025) and by fracture mechanics (Liu et al., 2009) and (Lotsberg, 2014) are only able to consider the geometrical size effect. The fracture mechanics simulations confirm that the smaller is the weld toe angle, the smaller is the size effect; however, the results depend largely on the assumptions of parameter values. As an example, Liu (Liu et al., 2009) concludes that the size exponent factor  $k = 0.2$  is too low, whereas Lotsberg (2014) concludes it is too high.

Pedersen (2019) evaluated various experimental campaigns, some of these showing a size effect related to specimen thickness, whereas others did not. He stresses the importance of the technological size effect based on the experimental work of (Ohta et al., 1990), where specimens tested with a stress ratio of  $R = 0$  did show a thickness dependency whereas specimens cycling down from yield and stress relieved specimens did not show a thickness dependency. Pedersen (2019) concludes that the size exponent factor of  $k = 0.2$  is too high. This finding is in line with most other experimental studies. Another important finding is that the thickness effect of thicker plates seems smaller than that of thinner plates in e.g. (Fukuoka and Mochizuki, 2010), where doubling and gusset plates with thickness of 25 and 50 mm were tested and almost no or even a positive thickness effect was observed. This finding is in line with Lotsberg (2014) and HSE (Health Safety Executives HSE OTH 92 390, 1999) who report tests on cruciform joints loaded in bending and tension, respectively, with  $R \approx 0$  having plate thicknesses ranging between  $20 \leq t \leq 150$  mm (both for the loaded plate and the attachment, with one test even with  $t = 200$  mm) that show practically equal fatigue resistance for  $t = 100$  mm and  $t = 150$  mm. All these findings support the conclusion that the technological size effect is dominant for butt welded joints, as a specimen of a certain thickness is already fully constrained against deformation during welding, and additional thickness does not further influence this.

A key limitation of size effect evaluation by experimental testing is the constrained range of specimen dimensions that can be practically investigated. The specimens reported in Lotsberg (2014) and HSE (Health Safety Executives HSE OTH 92 390, 1999) are the largest in size of all specimens found in the literature. In addition, because of the inherent scatter in the fatigue resistance, it is difficult to draw quantitative conclusions (Zhao and Hsu, 2020).

#### 2.4. Statistical size effect

Limited test data exist to evaluate the statistical size effect in fatigue of welded joints. Xiao and Yamada (2004) showed an effect of specimen length in tests with welded attachments, but their tests were limited to  $W \leq 200$  mm and the effect might be dominated by differences in residual stress caused by the constraints imposed (i.e. technological size effect). Butt welds in monopiles are much longer, yet, these are not the only connection types with long weld lengths. Longitudinal welds of pipes can be extremely long – these welds are transversely loaded by fluctuating pressure – and the same applies for the combined lengths of welds in orthotropic bridge decks of long span bridges. Comparably, in non-welded components, the stay, suspension, or mooring cables composed of parallel wires have a very long total wire length. In all of these cases, the structural length is many times larger than the length of specimens tested to establish the stress-life (S-N) curve.

Several methods exist to evaluate the statistical size effect of the weld length. Tao et al. (2024) quantified the probability of failure using the concept of highly stressed volume. A similar approach was adopted by Deinböck et al. for weld length effects using the effective notch stress concept (Deinböck et al., 2020). Paolino (2021) correlated the probability of failure with the largest defect size and stress range, and accounted for stress gradients. Worsman et al. (Wormsen et al., 2007) determined the probability of failure by correlating the stress field with

the critical defect distribution, making use of the Kitagawa-Takahashi diagram. These studies allow to consider the fact that the stress may not be of the same magnitude along the weld length, a situation that occurs in monopiles because of dominant wind directions. Moreover, these studies show that the length effect reduces with increasing length. The guideline DNV-RP-C203 (2025) proposes a reduction of the fatigue life  $\Delta N$  equal to:

$$\log_{10}(\Delta N) = 0.1 \cdot \log_{10} \left( \frac{W}{W_{ref}} \right) \quad (2)$$

where  $W_{ref}$  is the weld length applied in the fatigue tests. Some incomplete background of this correction is provided in (Valsgård et al., 2010). Using this proposal for an assumed  $W_{ref}$ , the fatigue resistance drops by 8%, 16% and 26% for a weld length  $W = 1$  m, 10 m and 100 m, respectively, if the weld is equally stressed along its full length.

Weibull distributions are often applied for weakest link processes. The fatigue test evaluation method of Castillo and Fernández-Canteli (2009) uses a Weibull distribution to fit fatigue test data and to describe length effects. In (Castillo et al., 1985), they applied their model to long cables and they showed that, under the hypothesis that their statistical model is correct, the length effect is important up to a certain length and that, with increasing length, the characteristic (i.e. lower bound) fatigue resistance is practically unaltered. This is because the mean fatigue life at given stress range reduces but so does the standard deviation.

Based on the above overview, the size exponent of  $k = 0.2$  in standards for butt welds is likely conservative when the thickness effect is taken into account. The philosophy of EN 1993-1-9 (prEN 1993-1-9:2025, 2025) has been that larger  $t$  often implies larger  $W$ , so that the (conservative) size exponent also covers for (a part of) the length effect. Further, there are indications that the size effect reduces (or may even be absent) towards very thick and long welds; yet, sufficient tests are lacking to confirm this.

#### 2.5. Misalignments

Axial and angular misalignments, which are schematically illustrated in Fig. 3, have a significant effect on the fatigue resistance of butt-welded joints. As a demonstration, Braun and Kellner (2022) evaluated 625 fatigue tests on thin-walled butt-welded joints ( $6 \leq t \leq 20$  mm) with machine learning and found that misalignment is the second most influential parameter affecting fatigue resistance, following stress range as the primary factor, and ranking above local geometrical parameters. The influence of misalignments depends on the constraints against out-of-plane deformation. Lotsberg (2009) mentions that angular misalignment has an important effect on small-scale specimens, but hardly on full-scale realistic structures due to the constraints that usually apply. Although this statement may not hold in general, it does apply to monopiles, where the curvature of the shell prevents (significant) angular misalignments during construction (at the cost of higher residual stress as described above). What remains is the axial misalignment, which can be caused by the tolerances in the positioning, the diameters and the shape (out-of-roundness) of the two cans. The curvature of the shell also reduces the effects of axial misalignments because of the constraint it imposes. The effects of it on pipes are quantified in studies through the stress concentration factors (Lotsberg, 2009) or stress intensity factors (Zhao et al., 2018). An insightful study into the curvature influence in shells can be found in (Ecker and Unterweger, 2023) where the effect of axial misalignments was studied for thickness transitions through the stress concentration factor. The study showed no effect of the curvature in the hot-spot stress and the effective notch stress for  $\frac{D}{t} > 100$ , indicating similarity with a flat plate for relatively large diameters. These stresses reduce rapidly with  $\frac{D}{t}$  for  $\frac{D}{t} < 100$ . In practice, monopile dimensions have increased significantly over the last decade, with typical sizes growing from outer diameters of 5–6 m and wall thicknesses of 55–85 mm ( $\frac{D}{t}$  of 60–110) in the 2010s to 8–9 m in

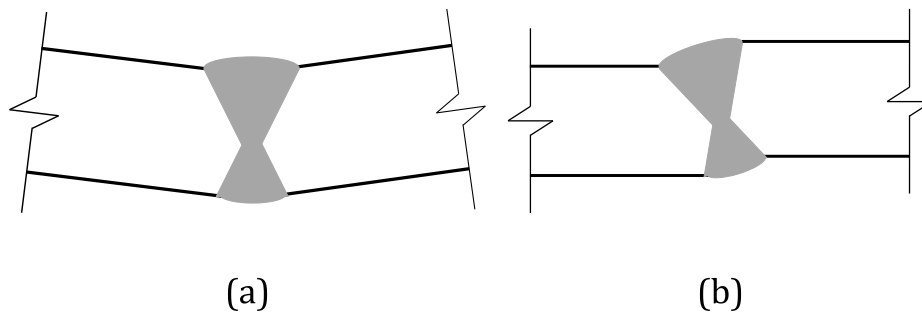


Fig. 3. Schematic illustration of (a) angular misalignment, (b) axial misalignment.

diameter and 67–90 mm in thickness ( $\frac{D}{t}$  of 90–130) as of now in current installations, and much larger thicknesses of up to 170 mm for the new designs (Mehmanparast and Lotsberg, 2025).

### 3. Analysis of fatigue resistance and thickness effects in monopile-representative materials

#### 3.1. Fatigue data from the European database and new studies on offshore wind related materials

The fatigue resistance of welded joints is typically determined through statistical evaluation of fatigue test data, represented as S-N curves and categorized into various fatigue design classes (FAT) based on the weld type and surface finish. This approach inherently accounts for typical and unavoidable geometric and metallurgic notches, surface imperfections, inner imperfections (such as pores and inclusions) and residual stresses, which are thus reflected in the derived design value in terms of the characteristic fatigue resistance  $\Delta\sigma_C$ . The European fatigue database for detail catalogue of EN 1993-1-9:2024 (prEN 1993-1-9:2025, 2025) comprises over 20,000 test data points (Deutscher Ausschuss für Stahlbau, 2024) covering different classes of welds. The database has been established on the basis of two German research projects and further studies (Feldmann et al., 2019; Bartsch et al., 2020, 2024, 2025; Maljaars and Euler, 2021; Ono et al., 2021; Garcia et al., 2018; Hrabowski et al., 2021) resulting in numerous re-evaluations of common fatigue details (Bartsch and Feldmann, 2018; Drebenstedt and Euler, 2018). Regarding butt-welded joints, a large amount of data is already collected from the literature and included in the European Database, see e.g. (Bartsch, 2026). This study addresses the fatigue behaviour of offshore wind turbine support structures, focusing on two-sided butt welds. Existing fatigue data, mainly forming the background of EN 1993-1-9, are largely based on older, manually welded specimens and conventional steel structures. Consequently, they insufficiently represent modern offshore applications that involve thicker plates, advanced steel grades, and automated welding processes such as SAW.

To overcome these limitations, the current work systematically expands the database to include recent fatigue test data that are more relevant to offshore wind applications, encompassing representative thickness ranges, materials and welding procedures. These additional datasets provide a more robust basis for assessing fatigue performance of joints characteristic for offshore wind turbine monopile support structures, as summarised in Table 1. It should be noted that some references provide characteristic values for steel grades, while others provide nominal values without clarification, so the type of available information varies in different sources.

The statistical evaluation of the test data is presented in Section 3.2, follows EN 1990 Annex D (EN, 1990-1, 2023) and gives the characteristic fatigue resistance  $\Delta\sigma_C$  with 95% survival probability, while the data have been re-evaluated using the approach detailed in DNV-RP-C203

Table 1

Expansion of the European fatigue database by including offshore wind-relevant materials test data.

Source	Stress Ratio R [-]	(Base Material) Yield Strength $R_{eH}/f_y$ [MPa]	Thickness $t$ [mm]
(Mehmanparast and Lotsberg, 2025; Mehmanparast et al., 2018, 2024)	0.10	401	50
Glienke et al. (2024)	0.30	335	40
(Braun et al., 2021; Braun and Kellner, 2022)	–1; 0; 0.5	329; 426; 454; 449; 537	10; 12; 16; 20
Knobloch et al. (2024)	0.2; 0.3; 0.5	341; 405;	25; 40
Knobloch et al. (2025)	–0.1; 0.1; 0.3	355	35

(DNV-RP-C203, 2025) in Section 3.3. Using test data to obtain the design value for the fatigue resistance provides a practical and widely accepted basis for applying the nominal stress concept within the fatigue verification. It allows an easy, straightforward fatigue design in daily engineering practice despite the complexity of fatigue behaviour in welded joints. A significant degree of data filtering and domain-specific evaluation was carried out to identify test data that are both suitable and representative for fatigue analysis of offshore wind monopile welded structures. The analyses conducted below not only highlight the influence of dataset composition on the derived fatigue resistance but also underlines the necessity of an application-specific evaluation framework. Such a framework provides a more reliable basis for the development of design recommendations and standards tailored to offshore wind monopile structures.

#### 3.2. Statistical evaluation of fatigue data according to EN 1993-1-9

##### 3.2.1. Statistical approach in EN 1993-1-9

When determining design values for fatigue detail categories, statistical methods must be employed to account for the inherent scatter of fatigue failures. The FAT class in EN 1993-1-9, which defines the fatigue resistance at  $2 \cdot 10^6$  cycles, is derived from a statistically determined S-N curve based on fatigue test series (EN 1990-1, 2023). A linear relationship (Basquin-type relation) is assumed between  $\log_{10}(\Delta\sigma)$  and  $\log_{10}(N)$ , where the parameters are determined by fitting the model to the experimental failure data only (i.e. run-outs are excluded). Equation (3) presents the corresponding regression function for fatigue analysis based on EN 1993-1-9 approach (prEN 1993-1-9:2025, 2025).

$$\log N = \log a - m \cdot \log \Delta\sigma \quad (3)$$

EN 1993-1-9 (prEN 1993-1-9:2025, 2025) defines the inverse slope  $m$  for S-N curves associated with butt welds by assigning a fixed value of  $m = 3$ . Alternatively, the true inverse slope of the curve can also be calculated and is then assigned  $m^*$ . The inverse slope  $m$  is fixed in EN

1993-1-9 (prEN 1993-1-9:2025, 2025), but the true inverse slope  $m^*$  can be determined (if desired) by:

$$m^* = \frac{\sum \log \Delta \sigma \log N - \frac{\sum \log \Delta \sigma \sum \log N}{n}}{\sum \log \Delta \sigma^2 - \frac{(\sum \log \Delta \sigma)^2}{n}} \quad (4)$$

Here,  $n$  represents the number of failed tests.

If  $m$  is predefined, only the intercept of the  $\log N$  axis, expressed as  $\log a$ , needs to be specified. The general formulation of this equation can be found in (Kosfeld et al., 2016):

$$\log a = \frac{1}{n} \sum_{i=1}^n \log N_i + m \cdot \frac{1}{n} \sum_{i=1}^n \log \Delta \sigma_i \quad (5)$$

To ensure safe design regulations, most data points must lie above a statistically determined design limit. Based on the fatigue test results, the prediction interval forecasts future test outcomes or design cases, if  $m$  is predefined (Meeker et al., 2017):

$$\log N_{p\%}^{\pm} = (\log a + m \cdot \log \Delta \sigma) \pm t \cdot \hat{s} \sqrt{1 + \frac{1}{n}} \quad (6)$$

Here,  $t$  represents the appropriate percentage point of Student's  $t$ -distribution, and  $\hat{s}^2$  is the best estimate of the variance of the data around the regression line. In investigations carried out in the present study, a one-sided prediction interval with a 95% confidence level is applied. This approach aligns with the statistical methodology outlined in Annex D of EN 1990-1 (EN 1990-1, 2023) and the background document to EN 1993-1-9 (Sedlacek et al., 2016).

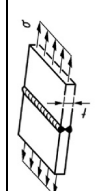

### 3.2.2. European fatigue database for two-sided butt welds

In this section, a comprehensive review of the existing European fatigue database, which forms the background for EN 1993-1-9 (prEN 1993-1-9:2025, 2025), is presented for the constructional detail “two-sided butt weld without post-weld treatment” for as-welded condition in air environment with the stress ratio of  $R \geq 0$  and axial loading condition. In EN 1993-1-9, this detail is assigned a FAT class of 90, including considerations of the size effect for plate thicknesses exceeding 25 mm. The details of FAT 90 class are summarised in Table 2. Comparable classifications and weld details are also provided in IIW (Hobbacher and Baumgartner, 2024) and, especially relevant for monopiles, in DNV-RP-C203 (2025) for double V-groove butt welds with as-welded condition.

In total over 4700 individual data points are included for butt welds in the existing European fatigue database without any judgment on the quality of the collated data. This includes various steels (such as austenitic steels, high strength steels, etc) as well as outliers, e.g. due to different failure position, imperfections of the weld and single sided butt welds. The full dataset is presented and analysed in Table 3. The dataset exhibits substantial scatter. After filtering for run-outs, failure from internal defects, post-weld treatment and outliers (such as weld imperfections), and including only structural steels, maximum fatigue life of  $5 \cdot 10^6$  cycles, double-sided welds, axial loading condition and  $R \geq 0$ , the qualified data from the European fatigue database is reduced to 1013 points for dataset number 1 (see Table 3). The results of the statistical evaluation are also presented in Table 3, with the inverse slope calculated using the linear regression analysis technique denoted  $m^*$ . For the predefined inverse slope of  $m = 3$ , the characteristic fatigue resistance is  $\Delta \sigma_C = 89 \text{ N/mm}^2$ , reflecting the large scatter in the dataset ( $\Delta \sigma_{C,50\%} = 139 \text{ N/mm}^2$ ). Based on the filtered data, the calculated inverse slope of the S-N curve is determined to be  $m^* = 2.46$ .

Regarding the assessment of offshore monopiles, the relevant application includes: thick plates, multi-pass welds, structural steel grade S355, and SAW. Using this information as additional filtering criteria to extract an offshore-relevant dataset, the European fatigue database is further refined, as summarised in Table 3. The first step involved splitting the data according to plate thickness, with a typical

**Table 2**  
Overview of investigated fatigue detail according to EN 1993-1-9 (prEN 1993-1-9:2025, 2025).

Detail category	Constructional detail	Symbol	Description	Requirements
90			Splices in plates and flats of same thickness, welded from both sides, as aforementioned, but as-welded with flank angle $\geq 150^\circ$	Welded in welding position PA acc. to EN ISO 6947. Weld ground flush at plate edges in direction of stress, where relevant, after removing weld run-off pieces. Misalignment $\leq 5\%$ of plate thickness, see NOTE 2.

NOTE 1 Size effect for  $t > 25$  mm is considered by stress modification with  $k_s = (25/t)^{0.2}$  for as-welded details where  $t$  is the plate thickness in mm for which the stress range is calculated.

NOTE 2 Misalignment due to fabrication  $\leq 5\%$  of plate thickness. An eccentricity is considered by appropriate nominal stress modification.

**Table 3**  
Statistical evaluation of fatigue tests for different data sets using the European database.

Dataset Number	Filtering Criteria	Mean FAT Class $m = 3$	Design FAT Class (EC3) $m = 3$	Calculated inverse slope	FAT Class for	Number of tests $n$
		$\Delta\sigma_{c,50\%}$	$\Delta\sigma_c$	$m^*$	$m^*$	
		[MPa]	[MPa]	[-]	[MPa]	[-]
1	- No runouts - No defects - No post-weld treatment - Max $5 \cdot 10^6$ cycles - Only structural steels - Welded from both sides - Axial loading condition - $R \geq 0$	136	89	2.51	88	1013
2	- Same Filter as in No. 1 - $t \geq 25$ mm	125	86	2.98	100	229
3	- Same Filter as in No. 1 - $t \leq 25$ mm	140	91	2.46	88	796
4	- Same filter as in No. 2 - Only S355	120	91	3.64	130	103
5	- Same filter as in No. 2 - Only Submerged arc welding	115	93	3.91	125	53
6	- Same filter as in No. 5 - Only S355	113	93	3.91	123	41

threshold of  $t = 25$  mm. This distinction is primarily reflected in the inverse slope parameter of the S–N curve, which increases from  $m^* = 2.46$  to 2.98 for specimens with  $t \geq 25$  mm (i.e. dataset number 2 in Table 3) and 2.46 for  $t \leq 25$  (i.e. dataset number 3 in Table 3), indicating a dependence of fatigue behaviour on thickness. Applying these thickness-based criteria along with other offshore-relevant filters, reduces the dataset to 229 points for thicker plates ( $t \geq 25$ ), while there were 796 points for thinner plates ( $t \leq 25$ ), thereby providing a more focused and representative basis for assessing fatigue performance in offshore wind turbine support structures.

Additional filtering of the dataset for S355 steel (dataset number 4 in Table 3), SAW (dataset number 5 in Table 3) and S355-SAW combined (dataset number 6 in Table 3) reveals that the resulting smaller database exhibits reduced scatter compared to the broader dataset. The characteristic fatigue resistance is approximately 93 N/mm<sup>2</sup> for these filtered datasets, while the inverse slope parameter of the S–N curve increases to  $m^* = 3.64$  for dataset number 4,  $m^* = 3.91$  for dataset number 5, and  $m^* = 3.91$  for dataset number 6. This indicates a large sensitivity of the dataset filtering criteria to the material and weld type. It should be noted

that the remaining data in these datasets after filtering are derived from only a few sources, emphasising the limited statistical basis for these results. The effect of the scatter band in the fatigue data remains significant. While the median fatigue resistance,  $\Delta\sigma_{c,50\%}$ , decreases slightly in datasets 4, 5 and 6, the characteristic fatigue resistance,  $\Delta\sigma_{c,m^*}$  increases significantly compared to set 1 and set 2. This observation underscores the importance of the consistency and quality of the underlying fatigue data for reliable design.

3.2.3. Combining new offshore wind monopile-related butt weld data with the European database

The new offshore wind monopile-related butt weld data are obtained from several sources, which are summarised in Table 1, with the new set of results obtained from the combination of the European fatigue database and new test data summarised in Table 4 and illustrated in Figs. 4–7. This includes 267 new datapoints (with 35 run-outs) from (Braun et al., 2021; Braun and Kellner, 2022), which were not previously included in the Eurocode fatigue database and cover plate thicknesses from 10 to 20 mm. In addition, 29 recent fatigue tests from

**Table 4**  
Statistical evaluation of fatigue tests for different data sets using the European database as well as newly added data according to Table 1.

No.	Filtering Criteria	Mean FAT Class $m = 3$	Design FAT Class (EC3) $m = 3$	Calculated	FAT Class $m^*$	Number of test, $n$	Figure
		$\Delta\sigma_{c,50\%}$	$\Delta\sigma_c$	Inverse slope $m^*$	$\Delta\sigma_c$		
		[MPa]	[MPa]	[-]	[MPa]	[-]	
1	- No runouts - No defects - no post weld treatment - max $5 \cdot 10^6$ cycles - only structural steels - welded from both sides - axial loading condition - $R \geq 0$ - new data added	130	84	2.32	75	1286	Fig. 4
2	- Same Filter as in No. 1 - $t \geq 25$ mm	122	86	2.97	96	295	Fig. 5
3	- Same Filter as in No. 1 - $t \leq 25$ mm	133	84	2.22	73	1013	Fig. 6
4	- Same filter as in No. 2 - Only S355	118	89	3.46	109	180	Fig. 7

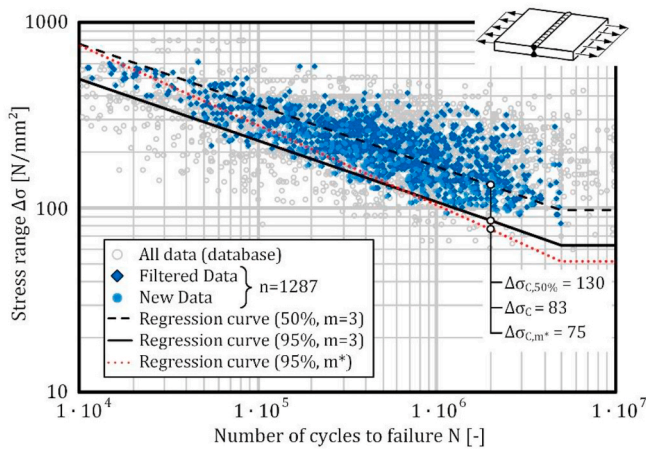


Fig. 4. Statistical evaluation of fatigue tests including European database in dark blue and newly added data in light blue in data set No. 1. (For interpretation of the references to colour in this figure legend, the reader is referred to the Web version of this article.)

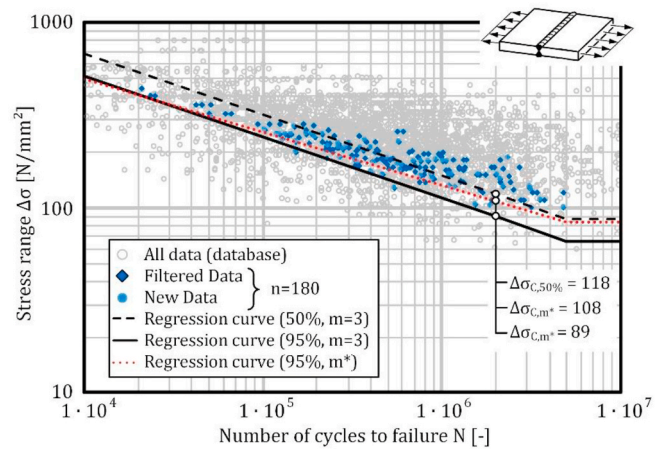


Fig. 7. Statistical evaluation of fatigue tests including European database in dark blue and newly added data in in data set No. 4. (For interpretation of the references to colour in this figure legend, the reader is referred to the Web version of this article.)

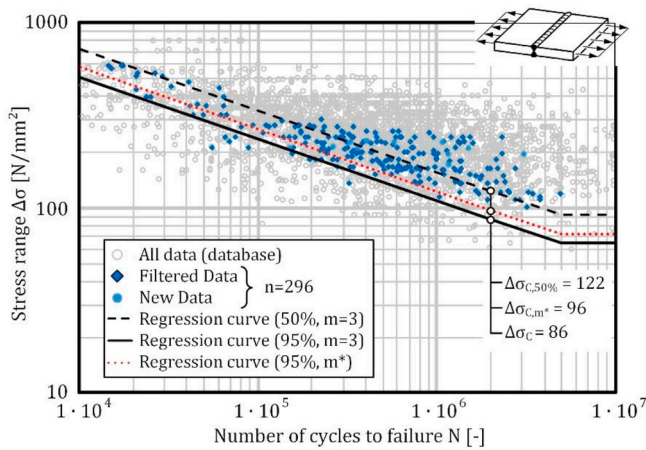


Fig. 5. Statistical evaluation of fatigue tests including European database in dark blue and in data set No. 2. (For interpretation of the references to colour in this figure legend, the reader is referred to the Web version of this article.)

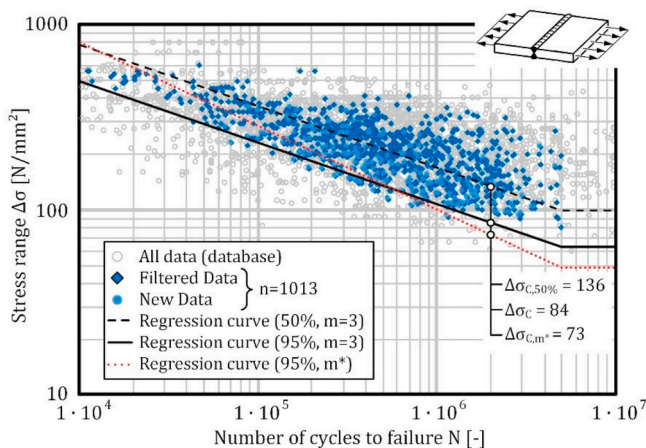


Fig. 6. Statistical evaluation of fatigue tests including European database in dark blue and in dataset No. 3. (For interpretation of the references to colour in this figure legend, the reader is referred to the Web version of this article.)

(Mehmanparast and Lotsberg, 2025; Mehmanparast et al., 2018, 2024) on 50 mm thick specimens feature double-sided butt welds made of S355 ML steel were added. Further contributions include 19 datapoints (including 1 run-out) for thick plates (40 mm, SAW, double V butt weld) extracted graphically from (Glienke et al., 2024), involving S355 J2+N steel with a SAW top layer, as well as relevant data from Knobloch (Knobloch et al., 2024) and Knobloch (Knobloch et al., 2025).

In Figs. 4–7, the newly incorporated data are highlighted in a lighter colour and predominantly occupy the lower bound of the dataset scatter, as seen in the figures. Statistical evaluation shows a slight reduction in fatigue resistance, a trend that holds across all applied filtering criteria, although the differences are not substantial. Adding these new data to the monopile-filtered dataset significantly increases the number of tests. The impact on the statistical evaluation is limited when assuming the predefined inverse slope of  $m = 3$ , whereas using the actual inverse slope derived from the data reveals a more pronounced effect on fatigue resistance, which subsequently influences the design fatigue resistance  $\Delta\sigma_{c,m^*}$ . The final filtered dataset, Table 4, which includes only thick plates ( $t \geq 25$  mm), positive stress ratios, and S355 steel specimens, exhibits a high characteristic fatigue resistance of  $108 \text{ N/mm}^2$  for  $m^*$ . The inverse slope of the S-N data derived from the linear regression analysis is  $m^* \approx 3.45$ , which closely matches the inverse slope presented in Appendix F.16 of DNV-RP-C203 (DNV-RP-C203, 2025), thereby confirming the consistency of the dataset with established offshore design standards.

The incorporation of monopile-related fatigue test data into the European fatigue database shows that relying on the unfiltered dataset leads to unprecise estimates of fatigue performance for butt joints characteristic for offshore wind turbine monopile support structures. Applying the appropriate filters for a specific application, in this case offshore wind monopiles, results in a significant reduction in scatter. The refined and expanded database offers stronger statistical reliability, lowers data scatter, and yields higher S-N inverse slopes together with higher characteristic strengths, thereby providing a more realistic representation of the behaviour of modern butt welds used in monopiles; however, a major limitation remains the lack of high-quality and well-documented experimental results for thick plates (particularly for  $t > 50$  mm), emphasising the need for targeted large-scale testing programmes that replicate monopile welding practices and operational conditions.

### 3.3. Re-evaluation of offshore monopiles related data using the DNV-RP-C203 approach

The offshore wind monopile related fatigue data presented above are re-evaluated in this section using the approach described in DNV-RP-C203 (DNV-RP-C203, 2025), which is the main guideline for the design of offshore wind turbine welded support structures. The as-welded condition in DNV-RP-C203 is described using the D curve, which is comparable to the FAT class 90 in EN 1993-1-9 exposed to air environment, which is also deemed applicable for coated surfaces in marine environment, provided the coating is undamaged. In DNV-RP-C203, the standard design curves for butt welds are specified for a reference thickness of  $t_{ref} = 25$  mm, with adjustments applied for butt welds exceeding this thickness using:

$$\log N = \log \bar{a} - m \cdot \log \left( \Delta \sigma \left( \frac{t_{eff}}{t_{ref}} \right)^k \right) \quad (7)$$

where  $m$  is the inverse slope of the S-N curve,  $\log \bar{a}$  is the intercept of the design S-N curve, which can be obtained using the following equation by employing the intercept of the mean curve  $\log a$  and the standard deviation  $s_{\log N}$ :

$$\log \bar{a} = \log a - 2 \cdot s_{\log N} \quad (8)$$

In Equation (7),  $k$  is the thickness exponent, which takes a value of 0.2 for the D-curve in air, and the effective thickness,  $t_{eff}$ , is determined using:

$$t_{eff} = \min [(14 + 0.66 \cdot L_t), t] \quad (9)$$

where  $L_t$  is the weld width and  $t$  is the plate thickness.

The monopile relevant fatigue data identified based on the filtering criteria number 4 explained in Tables 4 and is re-analysed in this section based on the DNV methodology described above. The results from the linear regression analyses, for the thickness values of 25, 30, 35, 40, 50, 60 and 80 mm are shown in Fig. 8, with the inverse slope  $m$ , intercept of the mean curve  $\log a$ , the standard deviation  $s_{\log N}$  and the number of test data available for each thickness  $n$  summarised in Table 5. In addition to the mean and lower bound (mean curve subtracted by two standard deviations) curves fitted to the data for each thickness, the thickness corrected D curve in air, calculated based on the monopile-specific guidelines in Appendix F.16 of 2024 version of DNV-RP-C203, is also included for comparison with the lower bound fit to the data. In calculation of the thickness corrected monopile-specific D curves, a fixed weld width to thickness ratio of  $L_t/t = 0.8$  was assumed for all thicknesses.

As seen in these figures, all of the test data at various thicknesses and their associated lower bound fits fall above the recommended thickness corrected monopile-specific D curve provided in DNV-RP-C203. The number of relevant test data for fatigue design of offshore wind monopiles, varies across different thicknesses. Among the thickness values considered in this study, the existing data on 40 mm and 50 mm are found to be the richest compared to other thickness values of  $t \geq 25$  mm, with the test data for both of these thickness values equally distributed across a wide range of  $\Delta \sigma$ . It is also worth noting that although 50 mm represents the lower bound of wall thickness for existing monopiles in the offshore wind industry and newer designs employ significantly greater thicknesses, the available experimental data for thicknesses exceeding  $t > 50$  mm remain sparse. In particular, there is a lack of data for representative weld types and qualities under axial loading conditions, as opposed to bending, for larger thicknesses. This scarcity highlights the critical need for additional testing on thicker welds to support and, if necessary, refine the thickness correction methodology specified in the DNV-RP-C203 standard for thicknesses well beyond the reference value of  $t_{ref} = 25$  mm detailed in the standard.

Fig. 8 also shows that, according to the DNV-RP-C203 standard, a

knee point is specified for the monopile-specific D curve at 3 million cycles, beyond which the inverse slope changes from 3.45 to 5.7 for the air environment. Given that under normal operational conditions, stress levels in large thickness offshore wind monopiles are relatively low, the region after the knee-point governs the majority of the structural lifetime where the main contribution to the accumulated fatigue damage takes place. However, the available monopile-representative data in Fig. 8 indicate that, apart from a limited number of data points at thicknesses of 40, 50, and 60 mm, there are insufficient experimental results in this region to enable a statistically robust evaluation of the inverse slope recommended after the knee-point in the standard. From an experimental perspective, it is important to note that S-N curve data are typically derived from laboratory tests conducted under constant amplitude loading, whereas offshore wind monopiles are subjected to variable amplitude loading in service. Constant amplitude testing often leads to an apparent endurance limit in the high cycle fatigue regime, below which no failures are observed and test results are reported as run-outs. Consequently, a key area for future research is the execution of variable amplitude fatigue tests on representative thick welds to properly characterise the high cycle fatigue behaviour of offshore wind support structures.

As seen in Table 5, the values of inverse slope generally vary between  $2.26 \leq m \leq 6.09$ , indicating fluctuations above and below the recommended inverse slope value of  $m = 3.45$  recommended for monopile-specific D curve in DNV-RP-C203 standard. Also seen in this table is that depending on the quality of the data available at different thicknesses, the standard deviation  $s_{\log N}$  variation has been found to range from 0.07 to 0.21. This shows that both the variation in the number of points and the range of  $\Delta \sigma$  over which the data points are distributed significantly influence the obtained results from the linear regression analysis for each dataset. Also, it is important to note that, whereas some of the data such as the ones available on the  $t = 50$  mm from (Mehmanparast and Lotsberg, 2025) are well documented with the misalignment corrections quantified and reported for each test, it is not possible to evaluate the quality of the data for the rest of the thicknesses to explore whether the global stress range values were reported or they were revised by considering misalignment corrections.

### 3.4. Analysis of the influencing factors on fatigue life

In this section, the offshore wind monopile related fatigue data presented above is re-analysed with a focus on specific influencing factors, including the potential effect of plate thickness, yield strength and the stress ratio. To enable a consistent comparison across all stress ranges, the fatigue test results have been normalized to the reference fatigue resistance at  $2 \cdot 10^6$  cycles using an inverse slope of  $m = 3$ . This normalization facilitates a systematic evaluation of trends, as illustrated in Fig. 9. The results obtained from the analysis on the filtered data from the European fatigue database combined with the new relevant fatigue test data presented in Fig. 9(a) indicates that the yield strength variation in different sub-grades of S355 steel does not exert a significant influence on the fatigue resistance while a small negative slope is observed in the analysis.

A detailed assessment of the thickness effect, presented in Fig. 9(b), reveals that when considering all available offshore wind monopile relevant data with the thickness of  $t \geq 25$  mm, a negative trend is observed, suggesting a potential thickness effect. As shown in Fig. 9(b), the slope of this trend is approximately parallel to the thickness modification factor of  $(t/25)^{0.2}$  recommended in EN 1993-1-9 guidelines; however, it is worth highlighting that when the test data for  $t = 25$  mm are excluded, the apparent negative effect of thickness disappears. This observation can be attributed to the significant level of scatter observed at each thickness value, making it challenging to accurately capture the impact of thickness increase on the fatigue life reduction and is in line with effects mentioned in Section 2 on absence or reduction of thickness effect based on very thick specimen tests. Fig. 9(b) indicates that the

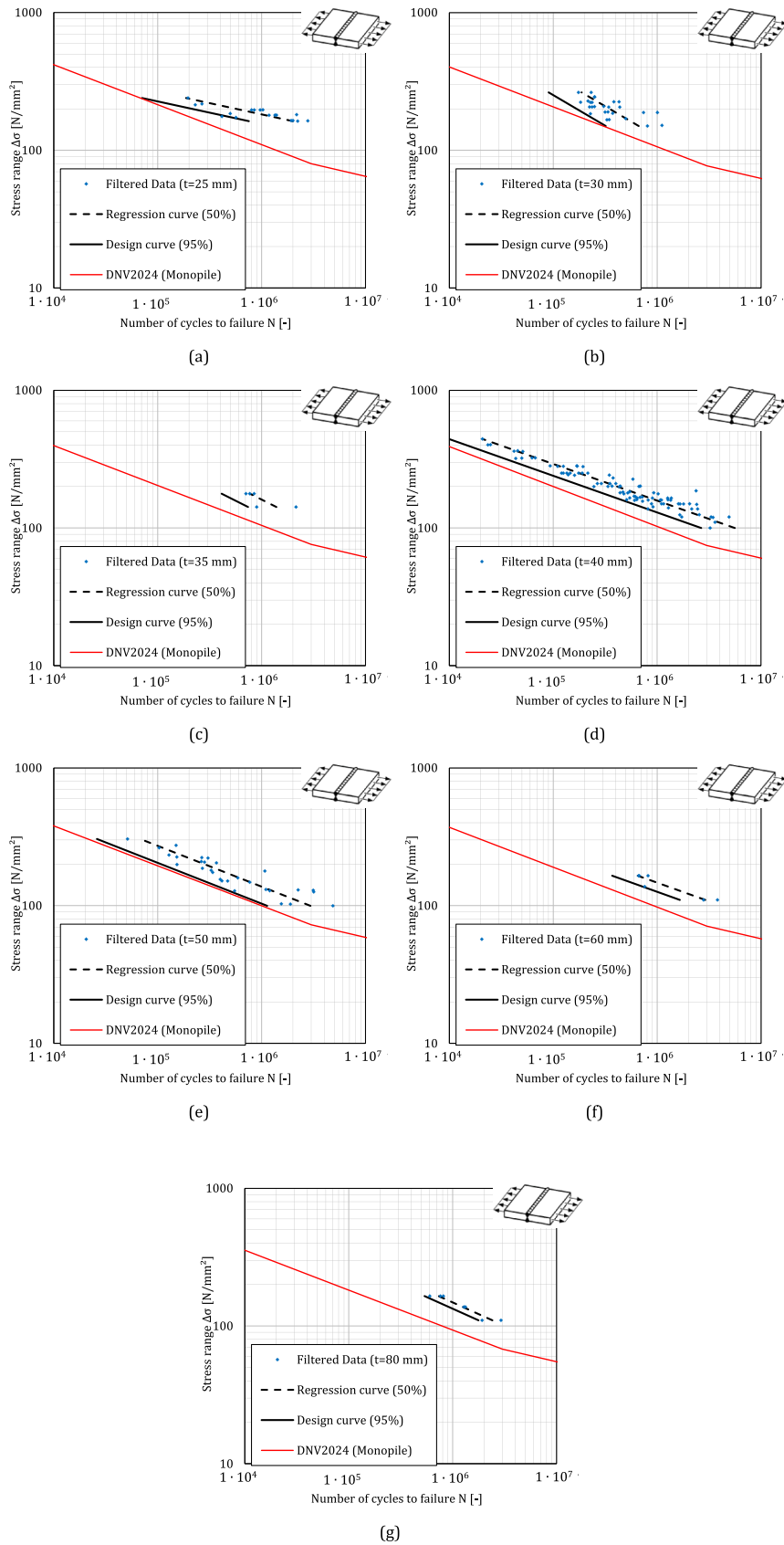


Fig. 8. Re-evaluation of the relevant fatigue data using DNV approach for thicknesses of (a) 25 mm, (b) 30 mm, (c) 35 mm, (d) 40 mm, (e) 50 mm, (f) 60 mm, and (g) 80 mm.

**Table 5**  
Summary of DNV evaluations of the monopile relevant fatigue data for different thicknesses.

No.	Filter Criterion: Thickness	Calculated inverse slope $m^*$	S-N mean curve intercept $\log a$	Standard deviation $s_{\log N}$	Number of tests $n$
1	$t = 25$ mm	6.09	19.7655	0.21	18
2	$t = 30$ mm	2.26	10.7338	0.16	27
3	$t = 35$ mm	2.62	11.7914	0.14	5
4	$t = 40$ mm	3.75	14.2511	0.16	86
5	$t = 50$ mm	3.37	13.2099	0.21	29
6	$t = 60$ mm	3.69	13.9972	0.12	6
7	$t = 80$ mm	2.94	12.3872	0.07	7

thickness trend in EN 1993-1-9 conservatively accounts for the fatigue life reduction as a result of increase in the plate thickness; however, it is important to note that the number of relevant fatigue test data for large thicknesses of  $t > 50$  mm are found to be very limited. Given that the wall thickness of circumferential welds in both current and future generations of offshore wind monopiles fall within this range, additional testing at large thicknesses is essential for future work. While some data are available for thicknesses up to 200 mm under bending fatigue loads, caution must be exercised when extrapolating these results to monopiles, where due the high diameter of the structures under bending fatigue cracks are predominantly driven by a low stress gradient close to pure axial loading. Using data from unrepresentative loading conditions could lead to inaccurate assessments of monopile fatigue performance.

Furthermore, the analysis in Fig. 9(c) shows that within the inherent experimental scatter the stress ratio has no influence on fatigue

performance of the offshore wind monopile related materials and welds for  $R \geq 0$ . While a very small positive trend line slope is observed in the analysis performed in Fig. 9(c), the influence of stress ratio on the fatigue life has been found to be negligible with no clear trend determined within the available data. The significant scatter in strength direction makes it virtually impossible to conclude on the effect of stress ratio. This highlights the need for additional tests of thick butt joints at different stress ratios. In addition, the missing influence of the stress ratio suggests the presence of tensile residual stresses, which is consistent with the expected high level of constraint for thick plates, as already mentioned in Section 2 and the often overly conservative assumption that welding related residual stresses are completely relaxed in small-scale fatigue test specimens.

These findings from these analyses suggest that, for the offshore wind monopile related fatigue test database considered in this study, moderate variations in neither yield strength nor  $R$ -ratio significantly compromise fatigue resistance, while the influence of thickness on fatigue life has been found to be more pronounced.

3.5. Discussion

The European fatigue database, which forms the basis of EN 1993-1-9, comprises over 20,000 fatigue data points, including more than 4700 for butt welds; however, a significant portion of these data originates from older test campaigns, often involving manual arc welding techniques and a wide variety of steel grades that do not correspond to current product standards in steel construction. When strict filtering criteria are applied to remove outliers, non-representative data, and non-structural steels, the number of relevant results is reduced to

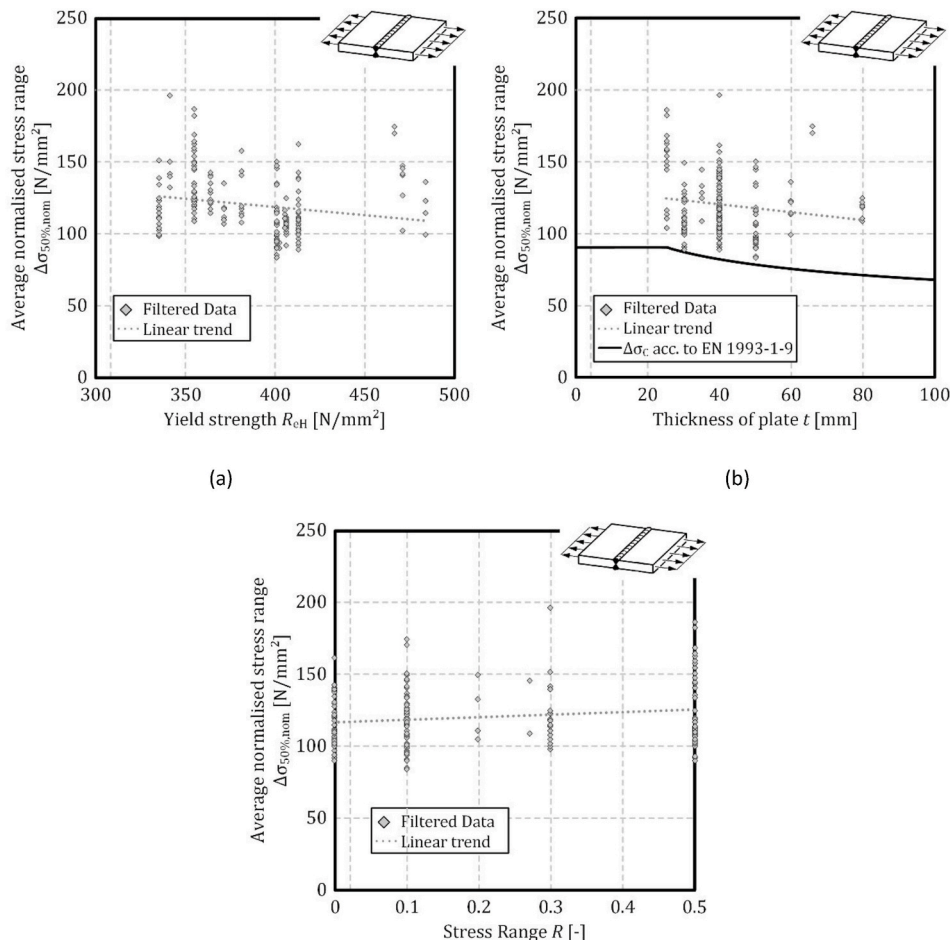


Fig. 9. Influence of yield strength, thickness and stress ratio on the fatigue life in offshore wind monopile relevant material data.

approximately 1100. The analysis of the filtered data from the European database on offshore wind welded structures relevant test data exhibits an inverse slope of  $m \approx 2.5$  in the S-N curve, which is lower than the typical value of  $m = 3$  recommended in standards for the low-to-medium cycle fatigue lives in welds.

For offshore monopiles, the relevant configuration typically involves thick plates with  $t \geq 25$  mm, S355 steel sub-grades, and double-sided SAW butt welds in as-welded condition (i.e. without post-weld treatment). By adding new relevant test data and combining them with the filtered data from the European fatigue database, it could be observed that the tailored database is reduced in size when the offshore wind welded structures related filters are applied, but its consistency and representativeness improve markedly. Notably, the re-calculated S-N inverse slope increases to  $m \approx 3.45$ , which indicates that unfiltered data with the typical inverse slope of  $m = 3$  tend to underestimate the fatigue life of offshore wind monopiles in medium-to-high cycle region.

The integration of newly available offshore wind related data, particularly for plate thicknesses of 40 and 50 mm, enhances the statistical robustness of the fatigue life analysis. Whereas these additional data, which did not exist in the European fatigue database, tend to cluster towards the lower bound of the existing scatter, hence slightly reducing the mean fatigue resistance, their inclusion confirms the characteristic resistances exceeding 100 MPa for conditions relevant to monopiles and a higher inverse slope  $m \approx 3.45$  compared to the typical value of  $m = 3$ , which is in excellent agreement with the newly introduced inverse slope of  $m = 3.45$  recently included in Appendix F.16 of the latest version of DNV-RP-C203 standard. This reinforces the conclusion that modern, carefully filtered data provide a more accurate representation of the fatigue performance of thick welded S355 joints in offshore welded structures.

A re-evaluation using the DNV-RP-C203 approach further supports these findings. All datasets for thicknesses between 25 mm and 80 mm lie above the DNV thickness corrected monopile-specific D curve, confirming the conservative nature of this design approach. The calculated inverse slope values for different thicknesses vary between 2.3 and 6.1 depending on dataset size and quality, yet the datasets on thickness values of 40 mm and 50 mm with sufficiently high number of data points consistently indicate inverse slope values of  $m > 3$ . Moreover, neither yield strength nor stress ratio  $R$  showed any influence on the fatigue performance of SAW welds in S355 structural steels, whereas more sensitivity to the plate thickness was found in data analysis. This indicates that within the observed experimental scatter, the material sub-grade (which is reflected in the yield strength sensitivity analysis) has negligible impact on fatigue resistance and the fatigue behaviour is dominated by weld geometry rather than slight variations in the yield strength of various sub-grades of S355 structural steel. While differences in yield strength are not covered by current standards, IIW-recommendation (Hobbacher and Baumgartner, 2024) provides an enhancement factor  $f(R)$  depending on  $R$  for components with low and moderate residual stresses; however, strict caution should be exercised when applying such correction factors, particularly for offshore wind monopile applications, as test data from large-thickness specimens indicate tensile residual stresses in the weld specimens, contradicting the assumptions of residual stress relaxation when cutting welded plates into small-scale fatigue test specimens.

A key limitation of the present study is that the analysis is restricted to positive stress ratios  $R \geq 0$ . This strategy was adopted in line with the conservative assumption of tensile residual stresses with magnitudes approaching the material yield stress being present throughout the lifetime of welded structure, which shifts the fatigue loading into an effective stress ratio of  $R \geq 0$ . Moreover, the presence of compressive stresses within fatigue cycles introduces additional complexity in data interpretation, as crack initiation and propagation are primarily driven by the tensile portion of the fatigue cycle, while compressive stresses promote crack closure and may reduce the effective crack driving force. By taking these considerations into account, the present study focuses on

establishing an S-N fatigue database for materials and welds representative of offshore wind monopiles under conditions of  $R \geq 0$ . The resulting baseline relationships can subsequently be adjusted using existing models and correction factors to account for the potential occurrence of negative stress ratios during operational loading. Consequently, further dedicated investigations are required to enhance the understanding of fatigue behaviour under  $R < 0$  conditions in monopile representative materials and welded joints.

In addition, it should be noted that the results presented here apply only to specimens tested in air. In reality, however, monopiles are protected against free-corrosion by means of cathodic protection (CP) in the sub-merged sections or surface coating in the splash zone region. For the free-corrosion environment, DNV-RP-C203 provides S-N curves with reduced fatigue strength, derived from the S-N curves in air environment, through the application of so-called environment reduction factors (ERF). The S-N curves in air are therefore considered the fundamental baseline, from which realistic adjustments can be made to account for actual operational and environmental conditions. The basis for these reductions lies in publications by the UK Health and Safety Executive (OTH 92 392, 1994; OTH 92 390, 1998) which compiled results from various research projects conducted in the 1980s. These studies indicated that the influence of CP is more pronounced in the finite-life regime than in the high-cycle regime. Accordingly, design ERF values of 2.5 for the finite-life regime (up to  $2 \cdot 10^6$  cycles) and 1.0 for the high-cycle regime (from  $10^7$  cycles onward) were defined, with a linear interpolation between the two limits. At the same time, the data revealed clear differences between various joint geometries. In particular, Solli (1981) reported very low ERF values for CP in butt welds, which, however, are not reflected in the design ERFs. The potential use of these lower ERF values for monopile design has not been fully clarified, as the experiments by Solli (1981) were conducted on 25 mm thick plates under bending loads only. In addition to the known differences between bending and axial loading, the interaction between CP and the thickness effect for butt-welded joints remains unexplored. Since addressing the environmental aspects would have exceeded the scope of this study, the present work focused solely on the thickness effect under air environment, as a baseline design, and further investigations will be carried out in future work to explore the environmental impacts on the design curves.

Overall, this study demonstrates that the unfiltered European database is not directly suitable for offshore wind applications, as it underestimates both characteristic fatigue resistances and S-N inverse slope for thick offshore wind welded structures. Targeted filtering and supplementation with new relevant test data produce more representative fatigue classes, reduce uncertainties, and show excellent agreement with DNV recommendations. Nevertheless, the limited availability of well-documented fatigue data for very thick structural steel plates under axial fatigue loading condition remains a significant source of uncertainty, underscoring the need for further experimental research specifically tailored to the geometries and loading conditions of offshore monopiles.

#### 4. Conclusions

This work studied the influence of thickness, length, stress ratio and yield stress variations on the fatigue performance of butt-welded joints relevant to offshore wind monopiles by systematically reviewing the literature and performing an updated statistical evaluation of fatigue test data from the European fatigue database, complemented with new data relevant to offshore wind welded structure-relevant datasets. The following conclusions can be made:

- The analysis shows that, while geometric considerations suggest thicker plates would have reduced fatigue resistance, the available experimental evidence indicates that the thickness correction applied in EN 1993-1-9 standard is conservative for butt-welded

joints, and more experimental data at thicknesses of  $t > 50$  mm would be required to confidently quantify the level of conservatism. Careful filtering of the database, focusing on steel grade S355, submerged arc welding, double-sided butt welds in as-welded condition in air with the load ratio of  $R \geq 0$  substantially reduces scatter and increases the inverse slope parameter of the S–N curve to  $m > 3$ , indicating improved fatigue behaviour in the medium-to-high cycle fatigue region under offshore-relevant fabrication conditions.

- The inclusion of recent fatigue test campaigns for thick plates further confirms the conservative nature of current design FAT classes, with characteristic fatigue resistance remaining close to FAT 90 or FAT 100 for thick plates ( $t \geq 25$  mm) with positive stress ratios, while the inverse slope parameter rises to  $m \approx 3.45$ , reflecting modern welding practices that produce smoother weld geometries and smaller imperfections.
- The obtained inverse slope of  $m \approx 3.45$  has been found to be in excellent agreement with the monopile-specific D curve in air recommended in Appendix F.16 of DNV-RP-C203 with all of the relevant test data at various thicknesses of  $25 \text{ mm} \leq t \leq 80 \text{ mm}$  falling above the thickness corrected monopile-specific S–N recommended in the same guidelines.

These findings demonstrate that the recent monopile-specific D curve in DNV-RP-C203 standard has proven to be safe for the specimens in the context of offshore monopiles, while the FAT classes in EN 1993-1-9 may result in over-conservative designs for the air environment. Also, this study highlights the importance of consistent databases and targeted data filtering when deriving design values for large-scale monopile butt welds. Remaining uncertainties include the limited availability of fatigue data for very thick plates ( $t > 50$  mm) under realistic offshore loading and welding conditions, emphasising the need for dedicated experimental campaigns, and the influence of local weld toe geometry, misalignments, and residual stresses, which remain critical for fatigue life and should be systematically considered alongside thickness effects. Overall, this work contributes to a better understanding of size effects on welded joint fatigue performance and offers a basis for further development of fatigue design methodologies for offshore wind support structures.

#### CRedit authorship contribution statement

**H. Bartsch:** Writing – original draft, Visualization, Validation, Resources, Methodology, Investigation, Formal analysis, Conceptualization. **S. Röscher:** Writing – original draft, Visualization, Resources, Methodology, Investigation, Formal analysis. **M. Braun:** Writing – original draft, Methodology, Investigation, Formal analysis. **J. Maljaars:** Writing – review & editing, Methodology, Investigation. **J. Schubnell:** Writing – review & editing, Methodology, Investigation. **M. Rauch:** Writing – review & editing, Investigation. **A. Chahardehi:** Writing – review & editing, Visualization, Validation, Methodology, Investigation. **A. Mehmanparast:** Writing – original draft, Visualization, Validation, Resources, Methodology, Investigation, Formal analysis, Conceptualization.

#### Declaration of competing interest

The authors declare that they have no known competing financial interests or personal relationships that could have appeared to influence the work reported in this paper.

#### Acknowledgement

The authors gratefully acknowledge the valuable discussions with Marc Seidel from Siemens Gamesa and Sulaiman Shojai from DLR, who provided important insights for this study.

#### References

- Bartsch, H., Feldmann, M., 2018. Assessment of fatigue tests to review detail categories of EC3. In: IABMAS. Melbourne, Australia.
- Bartsch, H. References European database [Online]. Available: [https://www.stahlbau.tsh.rwth-aachen.de/download/doc/LTT\\_References\\_Eurocepan\\_Database\\_v2.pdf](https://www.stahlbau.tsh.rwth-aachen.de/download/doc/LTT_References_Eurocepan_Database_v2.pdf) (Accessed: 23 January 2026).
- Bartsch, H., Seyfried, K., Seyfried, B., Feldmann, M., Kuhlmann, U., Ummehofer, T., 2020. Analysis of fatigue test data to reassess EN 1993-1-9 detail categories. *Steel Construction* 13 (4), 280–293.
- Bartsch, H., Seyfried, B., Hofmann, G., Feldmann, M., Ummehofer, T., Kuhlmann, U., 2024. Bewertung wesentlicher Einflussgrößen auf die Ermüdungsfestigkeit typischer Kerbdetails – experimentelle Untersuchungen. *Stahlbau* 93, 1–13.
- Bartsch, H., Feldmann, M., Seyfried, B., Ummehofer, T., Hofmann, G., Kuhlmann, U., 2025. Bewertung wesentlicher Einflussgrößen auf die Ermüdungsfestigkeit typischer Kerbdetails – bemessungsempfehlungen. *Stahlbau* 94 (10).
- Berge, S., 1984. Effect of plate thickness in fatigue design of welded structures, paper number: OTC-4829-MS. In: *Offshore Technology Conference*, Houston, Texas; USA.
- Berge, S., 1985. On the effect of plate thickness in fatigue of welds. *Eng. Fract. Mech.* 21 (2), 423–435.
- Braun, M., Kellner, L., 2022. Comparison of machine learning and stress concentration factors-based fatigue failure prediction in small-scale butt-welded joints. *Fatigue Fract Eng M* 45, 3403–3417.
- Braun, M., Kahl, A., Willems, T., Seidel, M., Fischer, C., Ehlers, S., 2021. Guidance for material selection based on static and dynamic mechanical properties at sub-zero temperatures. *J. Offshore Mech. Arctic Eng.* 143, 1–45.
- Castillo, E., Fernández-Canteli, A., 2009. A Unified Statistical Methodology for Modeling Fatigue Damage. Springer Science + Business Media B.V. springer.com.
- Castillo, E., Fernández-Canteli, A., Esslinger, V., Thürlimann, B., 1985. Statistical models for fatigue analysis of wires, strands and cables. *IABSE Proceedings* 82, 1–140.
- Deinböck, A., Hesse, A.-C., Wächter, M., Hensel, J., Esderts, A., Dilger, K., 2020. Increased accuracy of calculated fatigue resistance of welds through consideration of the statistical size effect within the notch stress concept. *Weld. World* 64, 1725–1736.
- Deutscher Ausschuss für Stahlbau (DASt). Ermüdungsversuchsdatenbank, 2024. <https://data.deutscherstahlbau.de/> [Online].
- DNV-RP-C203, 2025. Fatigue Design of Offshore Steel Structures. Det Norske Veritas, Edition, 10.
- Drebenstedt, K., Euler, M., 2018. Statistical Analysis of Fatigue Test Data according to Eurocode 3. In: *Proceedings of IABMAS 2018*. Melbourne.
- Ecker, A., Unterwiesing, H., 2023. Different fatigue design stress methods for common constructional details in cylindrical shells under axial loading – influence of the r/ratio and the shell thickness. *ce/papers* 6 (3–4), 2475–2482.
- EN 1990-1, 2023. Basis of Structural and Geotechnical Design. Brussels.
- European Commission, “The European Green Deal,” Brussels, 2019.
- Farajian, M., Nitschke-Pagel, T., 2015. Residual stress relaxation in welded large components. *Materialprüfung/Materials Testing* 57 (9), 750–754.
- Feldmann, M., Bartsch, H., Kuhlmann, U., Drebenstedt, K., Ummehofer, T., Seyfried, B., 2019. Auswertung von Ermüdungsversuchsdaten zur Überprüfung von Kerbfallklassen nach EC3-1-9. *Stahlbau* 88 (10), 1004–1017.
- Feldmann, M., Bartsch, H., Ummehofer, T., Seyfried, B., Kuhlmann, U., Hofmann, G., 2024. “EVOKERB – Evolution Kerbfalkatalog für wirtschaftlich optimierte Stahlbauten („Systematische Neubewertung wesentlicher Einflussgrößen der Ermüdungsfestigkeit nach Eurocode”) – IGF-Vorhaben Nr. 21368 N – Abschlussbericht. Stahlbau Verlags- und Service GmbH. Düsseldorf (in Bearbeitung).
- Fraunhofer, 2021. Offshore Wind as a cornerstone of the European Green Deal – the potential in upscaling production and utilization. *Fraunhofer Green Deal Series – Impulse*.
- Fukuoka, T., Mochizuki, K., 2010. Effect of Plate Thickness on Fatigue Strength of Typical Welded Joints for a Ship Structure, XIII-2vols. 333–10. IIW.
- García, M., Baptista, C.A.P., Nussbaumer, A., 2018. Multiaxial fatigue study on steel transversal attachments under constant amplitude proportional and non-proportional loadings. In: *12th International Fatigue Congress (FATIGUE 2018)*. Online.
- Glienke, R., Kalkowsky, F., Hobbacher, A.F., Holch, A., Thiele, M., Marten, F., Kersten, R., Henkel, K.M., 2024. Evaluation of the fatigue resistance of butt welded joints in towers of wind turbines – a comparison of experimental studies with small scale and component tests as well as numerical based approaches with local concepts. *Weld. World* 68, 1143–1168.
- Gurney, T.R., 1979. The influence of thickness on the fatigue strength of welded joints. In: *2nd Int. Conf. Behaviour of Offshore Structures (BOSS’79)*. London.
- Health Safety Executives HSE OTH 92 390, 1999. Background to new fatigue guidance for steel joints and connections in offshore structures. *Offshore Technology Report*. London, UK.
- Hobbacher, A.F., Baumgartner, J., 2024. Recommendations for Fatigue Design of Welded Joints and Components. Springer Nature Switzerland.
- Hrabowski, J., Herion, S., Ummehofer, T., Ladendorf, P., Pijpers, R., 2021. Erweiterung der Ermüdungsbemessung von K-Knoten aus Hohlprofilen. *Stahlbau* 90 (9).
- Knobloch, M., Rauch, M., Röscher, S., 2024. Ermüdung von Gurtdickensprüngen geschweißter Träger mit Stegausschnitt (FATTgirder), Deutscher Ausschuss Für Stahlbau DASt: Final Report IGF Nr. 21739 N.
- Knobloch, M., Rauch, M., Bissing, H., 2025. Prognosemodelle zur Lebensdauer und zum Weiterbetrieb von Windenergieanlagen (FutureWind), Forschungsvereinigung Stahlanwendung e.V.: Final Report IGF Nr. 20987 N.
- Kosfeld, R., Ecker, H.F., Türck, M., 2016. *Deskriptive Statistik*, 6 ed. Springer Gabler, Wiesbaden.

- Liu, G., Huang, Y., Wu, K., Lan, J., 2009. Fatigue strength assessment of extra thick welded joints in offshore structures. In: International Offshore and Polar Engineering Conference. Osaka, Japan.
- Livieri, P., Tovo, R., 2025. On the fatigue design strength of steel butt welded joints: size and geometrical effects. *Int. J. Fatig.* 199.
- Lotsberg, I., 2009. Stress concentrations due to misalignment at butt welds in plated structures and at girth welds in tubulars. *Int. J. Fatig.* 31 (8–9), 1337–1345.
- Lotsberg, I., 2014. Assessment of the size effect for use in design standards for fatigue analysis. *Int. J. Fatig.* 66, 89–100.
- Maljaars, J., Euler, M., 2021. Fatigue S-N curves of bolts and bolted connections for application in civil engineering structures. *Int. J. Fatig.* 151.
- Mancini, F., Remes, H., Romanoff, J., Goncalves, B.R., 2020. Stress magnification factor for angular misalignment between plates with welding-induced curvature. *Weld. World* 64, 729–751.
- Meeker, W.Q., Hahn, G.J., Escobar, L.A., 2017. *Statistical Intervals - a Guide for Practitioners and Researchers*, second ed. Wiley.
- Mehmanparast, A., Lotsberg, I., 2025. Advances in fatigue design of circumferential welds in offshore wind turbine monopile support structures. *Eng. Struct.* 337, 1–14.
- Mehmanparast, A., Taylor, J., Brennan, F., Tavares, I., 2018. Experimental investigation of mechanical and fracture properties of offshore wind monopile weldments: SLIC interlaboratory test results. *FFEMS* 41 (12), 2485–2501.
- Mehmanparast, A., Chahardehi, A., Brennan, F., Manzocchi, M., 2024. Re-evaluation of fatigue design curves for offshore wind monopile foundations using thick as-welded test specimens. *Eng. Fail. Anal.* 158.
- Ohta, A., Mawari, T., Suzuki, N., 1990. Evaluation of effect of plate thickness on fatigue strength of butt welded joints by a test maintaining maximum stress at yield strength. *Eng. Fract. Mech.* 37 (5), 987–993.
- Ono, Y., Baptista, C., Kinoshita, K., Yildirim, H.C., Nussbaumer, A., 2021. A reanalysis of fatigue test data for longitudinal welded gusset joints in as-welded and high frequency mechanical impact (HFMI)-treated state. *Int. J. Fatig.* 149.
- OTH 92 390, 1998. Background to New Fatigue Guidance for Steel Joints and Connections in Offshore Structures.
- OTH 92 392, 1994. A Survey of Some Recent Corrosion Fatigue Tests on Welded Joints in Steel Plate.
- Paolino, D.S., 2021. Very high cycle fatigue life and critical defect size: modeling of statistical size effects. *Fatig. Fract. Eng. Mater. Struct.* 44, 1209–1224.
- Pedersen, M.M., 2019. Thickness effect in fatigue of welded butt joints: a review of experimental works. *International Journal of Steel Structures* 19, 1930–1938.
- pEN 1993-1-9:2025, 2025. Eurocode 3: Design of Steel Structures – Part 1-9: Fatigue.
- Sedlacek, G., Hobbacher, A., Nussbaumer, A., Stötzel, J., Schäfer, D., Citarelli, S., Eichler, B., Feldmann, M., 2016. "Commentary to Eurocode 3: EN 1993 – Part 1-9 – Fatigue," Institut für Stahlbau und Lehrstuhl für Stahlbau und Leichtmetallbau der RWTH Aachen University, Aachen. (unveröffentlicht).
- Shams-Hakimi, P., Yildirim, H.C., Al-Emrani, M., 2017. The thickness effect of welded details improved by high-frequency mechanical impact treatment. *Int. J. Fatig.* 99 (1), 111–124.
- Solli, O., 1981. Corrosion fatigue of weldments of C-Mn steel: the effect of cathodic protection, stress relieving treatment and saline atmosphere. In: SIMS Conference. Paris.
- Tao, Z.-Q., Wang, Z., Pan, X., Su, T., Long, X., Liu, B., Tang, Q., Ren, X., Sun, C., Qian, G., Hong, Y., 2024. A new probabilistic control volume scheme to interpret specimen size effect on fatigue life of additively manufactured titanium alloys. *Int. J. Fatig.*
- United Nations, Department of economic and social affairs, sustainable development, "The 17 goals," [Online]. Available: <https://sdgs.un.org/goals>. [Accessed 21 August 2025].
- Valsgård, S., Lotsberg, I., Sigurdsson, G., Mørk, K., 2010. Fatigue design of steel containment cylinders for CNG ship application. *Mar. Struct.* 23 (2), 209–225.
- Wind Europe, 2025. *Wind Energy in Europe: 2024 Statistics and the Outlook for 2025-2030*.
- Wormsen, A., Sjödin, B., Härkegard, G., Fjeldstad, A., 2007. Non-local stress approach for fatigue assessment based on weakest-link theory and statistics of extremes. *Fatig. Fract. Eng. Mater. Struct.* 30, 1214–1227.
- Xiao, Z.-G., Yamada, K., 2004. A method of determining geometric stress for fatigue strength evaluation of steel welded joints. *Int. J. Fatig.* 26 (12), 1277–1293.
- Zhao, W., Hsu, W.-T., 2020. Re-Evaluation of fatigue thickness effect based on fatigue Test database. *J. Mar. Sci. Eng.* 8 (895), 1–25.
- Zhao, H.-S., Lie, S.-T., Zhang, Y., 2018. Fatigue assessment of cracked pipes with weld misalignment by using stress intensity factors. *Int. J. Fatig.* 116, 192–209.